

Acoustic Individual Identification of White-Faced Capuchin Monkeys Using Joint Multi-Species Embeddings

Anonymous ACL submission

Abstract

Acoustic individual identification of wild animals is an essential task for understanding animal vocalizations within their social contexts, and for facilitating conservation and wildlife monitoring efforts. However, most of the work in this space relies on human efforts, as the development of methods for automatic individual identification is hindered by the lack of data. In this paper, we explore cross-species pre-training to address the task of individual classification in White-Faced Capuchin monkeys. Using acoustic embeddings from birds and humans, we find that they can be effectively used to identify the calls from individual monkeys. Moreover, we find that joint multi-species representations can lead to further improvements over the use of one representation at a time. Our work demonstrates the potential of cross-species data transfer and multi-species representations, as strategies to address tasks on species with very limited data.

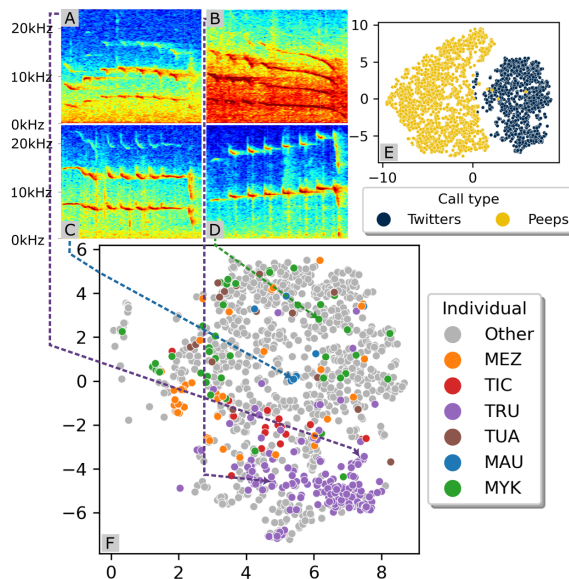


Figure 1: (A–D) Capuchin Twitter vocalizations show diverse structural variations. (E–F) t-SNE of Google Perch-Whisper embeddings. (E) Call type clusters. (F) Colored by individual, highlighting four diverse examples of Twitters.

1 Introduction

For a long time, researchers viewed the vocalizations of non-human species as mere reactions to internal emotional states (Lorenz, 1952). Consequently, early scientific methods in animal communication research largely overlooked individual differences and did not test for the presence of linguistic features (e.g., pragmatics, semantics, syntax) in animal communication systems. This simplified view of animal communication has been overturned by the growing evidence uncovering the presence of linguistic features in non-human animals (Bergman et al., 2019), leading to the emergence of Animal Linguistics as a formal interdisciplinary research field (Bowling and Fitch, 2015; Engesser et al., 2015; Suzuki, 2024; Berthet et al., 2023; Suzuki, 2021; Scott-Phillips and Heintz, 2023). This shift in perspective highlights the need for individual-level analysis, as it

allows researchers to account for the social and environmental contexts in which vocalizations occur, ultimately improving our ability to test their linguistic capacities more rigorously.

Additionally, long-term, individual-level analyses are critical for understanding and protecting wildlife. Such analyses support key approaches like social network quantification, assessing animal cognition, and performing capture–recapture techniques for tracking population dynamics (Slater, 1981; Carlson et al., 2020). Over the past decade, acoustic monitoring has emerged as a widely adopted, cost-efficient strategy in conservation, leading to growing interest in acoustic individual identification. By enabling researchers to recognize individuals from their vocalizations, this approach paves the way for more nuanced insights into ecology, behavior, evolution, and conservation (Knight

et al., 2024).

In this paper, we address the task of acoustic individual identification (Acoustic ID) in White-Faced Capuchins. We collect a two-year dataset of individualized focal recordings, a labor-intensive yet optimized method that mitigates signal-to-noise and cocktail party problems in wild bioacoustic settings (Bermant, 2021; Miron et al., 2024). Using this dataset, we evaluate human speech- and bird bioacoustic-based pre-trained networks, comparing single-embedding models to ensembles that merge embeddings from distinct networks. We hypothesize that human speech embeddings, such as Whisper or HuBERT, complement bioacoustic embeddings like Google Perch or BirdNET—originally trained on bird sounds—and predict that heterogeneous embedding combinations will outperform single-embedding models.

Transfer learning has significantly advanced acoustic classification tasks in non-human animals (Miyaguchi et al., 2024; Kahl et al., 2023; Abzaliyev et al., 2024). Recent studies on gibbons have explored the use of self-supervised speech models (e.g., HuBERT, Wav2vec 2.0), pre-trained bird classifiers (e.g., BirdNET, Perch), and non-transfer-learning deep models for primate Acoustic ID, finding that speech models most effectively capture individual vocal signatures, bird classifiers perform well in automated detection but are more susceptible to background noise, and non-transfer-learning models struggle when trained on small datasets (Cauzinille et al., 2024; Clink et al., 2024). Nevertheless, it remains unclear whether using multiple joint embeddings leads to better performance by exploiting complementary features from different training data domains.

This work makes three main contributions. First, we propose White-Faced Capuchin monkeys as a model organism for advancing computational research on animal communication. Second, we show that combining embeddings from human speech and bird bioacoustics models significantly improves acoustic identification performance in White-Faced Capuchins, outperforming single-embedding baselines. Finally, our findings show that acoustic diversity and soundscape similarity play a greater role than phylogenetic proximity. Smaller models trained on diverse bird vocalizations recorded in natural environments outperform much larger speech-trained models designed for humans, despite humans being more closely related to our study species. These results highlight the value

of cross-species model development in achieving better generalization for the Acoustic ID task.

2 Study system: White-Faced Capuchin Monkeys in the Taboga Reserve, Costa Rica

White-Faced Capuchin Monkeys (*Cebus capucinus*) are ideal for studying animal communication, with 27 call types (Gros-Louis et al., 2008), complex social behavior and cognition including tool use (Goldsborough et al., 2024), complex social networks (Crofoot et al., 2011) and cultural transmission (Perry et al., 2017). Taboga hosts their highest known density (Tinsley Johnson et al., 2020).

Data collection. Our field team collected audio recordings of focal individuals by following them in the Taboga forest. We used directional microphones aimed at the subjects from January 2021 to December 2022 through the wet and dry seasons, with hours ranging from 5 am to 5 pm. Recordings were captured at 48 kHz and 16 bit resolution. These raw recordings were subsequently trimmed to isolate the precise moments when vocalizations were detected, and only the calls classified as either a “Peep” or “Twitter” were included in this dataset, according to established criteria in the literature (Gros-Louis et al., 2008).

Audio recordings. The full dataset consists of 1,257 Twitter recordings and 2,089 Peep recordings from 45 individuals, although 15% of the recordings were assigned to unknown individuals. We include data from individuals that had at least 30 recorded calls, while recordings from unidentified subjects encountered in the field are grouped into an “Unknown” class. For Peeps, this dataset includes 15 individuals, and for Twitters this dataset included 10 individuals (total sample=1609). Peep calls are typically short (mean 0.27 s, SD 0.27 s), whereas Twitter calls are more complex (Figure 1) and longer (mean 0.40 s, SD 0.18 s).

3 Cross-Species Embeddings for Individual Classification

Collecting focal audio recordings of wild animals in their natural habitat is a challenging and resource-intensive task. Even with dedicated field teams, building large enough datasets to fully exploit deep neural networks is difficult. As a result, transfer learning—which leverages the induc-

159 tive bias of models pre-trained on larger, related
 160 datasets—has emerged as the most effective strategy
 161 for achieving high performance in bioacoustic clas-
 162 sification under low-data conditions (Ghani et al.,
 163 2023a).

164 **Audio Representation Models.** We extract pre-
 165 trained embeddings from Google Perch V8 (Ghani
 166 et al., 2023a), a model primarily trained on bird
 167 vocalizations, and Whisper (Radford et al., 2022),
 168 which was predominantly pre-trained on human
 169 speech. While additional embeddings were evalu-
 170 ated, we focus on these two in the main text for
 171 clarity, with results from five other models detailed
 172 in Appendix A. We apply mean-pooling to ob-
 173 tain lower-dimensional representations from large
 174 speech models like Whisper.

175 **Minimum Redundancy Maximum Relevance.**
 176 To combine representations from multiple species,
 177 we explore a feature-select model using Minimum
 178 Redundancy and Maximum Relevance (MRMR)
 179 (Ding and Peng, 2005), alongside simple concatena-
 180 tion and summation. Originally developed in can-
 181 cer research for gene selection, MRMR improves
 182 feature selection in high-dimensional datasets by
 183 balancing two key criteria: maximizing relevance
 184 to the target variable (measured via mutual informa-
 185 tion) while minimizing redundancy (filtered using
 186 a correlation coefficient threshold). Our implemen-
 187 tation starts with the feature that has the highest
 188 mutual information among both embeddings, re-
 189 moves any features with a correlation coefficient of
 190 0.8 or higher, and then iteratively selects the next
 191 most informative feature. This process continues
 192 until 1024 embedding features are selected from
 193 both embeddings, ensuring an optimal balance of
 194 diversity and informativeness.

195 **Experimental Setup.** To ensure a fair compar-
 196 ison, we carefully control parameter counts and
 197 apply hyperparameter tuning. Single-embedding
 198 models and the MRMR model compress each in-
 199 put into 512 units, then reduced it to 64 for fi-
 200 nal classification. Concatenation and summation
 201 ensembles apply a 256-dimensional compression
 202 to each embedding separately, then sum or con-
 203 catenate the outputs before another 64-unit layer.
 204 For a robust comparison, we generate 50 random
 205 train-test splits (10 recordings per individual in
 206 the test set) and train models with all seven sin-
 207 gle embeddings as well as all pairwise combina-
 208 tions (concatenation, summation, and MRMR).

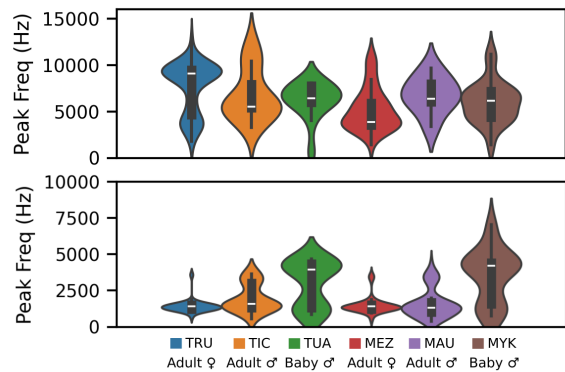


Figure 2: Peak frequency for the Peeps call type recordings of six capuchin monkey individuals

209 To identify the best hyperparameters for each
 210 model trained, we conduct a search over learn-
 211 ing rates $\{1e-5, 5e-5, 1e-4, 5e-4, 1e-3, 5e-3\}$ and
 212 dropout rates $\{0.2, \dots, 0.6\}$, evaluating 30 ran-
 213 domly sampled configurations for 100 epochs each
 214 with early stopping (patience=10, $\min \Delta F1=0.001$),
 215 and selected the highest F1-scoring setup. All mod-
 216 els are trained using the Adam optimizer. After
 217 confirming normality and homoscedasticity, we
 218 compare each architecture’s top-performing model
 219 via ANOVA and a post-hoc Tukey test.

220 **Spectrogram annotations and measurements.**
 221 To compare explainable acoustic features with non-
 222 interpretable deep embeddings, we manually mea-
 223 sure Peak Frequency and other acoustic parameters
 224 from spectrograms, following standard bioacoustic
 225 methods. Using Raven Pro 1.6 (K. Lisa Yang Cen-
 226 ter for Conservation Bioacoustics at the Cornell
 227 Lab of Ornithology, 2024), we select regions of
 228 interest and extract 30 interpretable features (see
 229 Appendix A), including Peak Frequency, Center
 230 Frequency, and Center Time. These measurements
 231 were taken from six individuals—one adult male,
 232 one adult female, and one infant from each of the
 233 two monkey troops—chosen for their distinct char-
 234 acteristics.

4 Results

235
 236 Table 1 shows the results of the Acoustic ID task
 237 for selected models. We present F1 scores for the
 238 models trained on bird vocalizations and human
 239 speech data, together with their ensembles. While
 240 single-species vocalization models perform reason-
 241 ably well, the models with the highest F1 scores
 242 are those that combine multiple embeddings (either
 243 using summation, concatenation or MRMR). Fur-

thermore, the best-performing ensemble combine models developed for bioacoustic vocalizations and models developed for human speech. This highlights the potential of cross-species pre-training in a limited data regime. Pre-training on human speech does not capture enough information for the bioacoustic domain, as shown by the performance of Whisper for both vocalization types. But combined, those two models achieve an F1 score of 0.70 for Peeps and 0.66 for Twitters. This improved performance suggests that combining speech-trained and bioacoustic-trained embeddings effectively leverages complementary information. We also present the results for other models in Appendix A.

Despite its smaller size and more limited training dataset, the bioacoustic model Perch outperforms the much larger Whisper model, which was developed for human speech. Domain relevance is more important than model size, training data set size, or phylogenetic proximity for the Acoustic ID task in Capuchins. Trained on data from noisy field conditions, Perch learns the acoustic variability of field conditions, contributing to its strong performance. Although our focal species is neither a bird nor a human, the top-performing models across architectures are trained using both bird- and human-derived embeddings, suggesting that joint multi-species embeddings provide better generalization for Capuchin acoustic classification tasks.

We visualize the embeddings of the best-performing model from table 1 using t-SNE (van der Maaten, 2009) in Figure 1. Different call types formed well-defined clusters (Figure 1E), whereas individual classifications appear more diffuse (Figure 1F), illustrating the difficulty of the Acoustic ID task (see A for more t-SNE visualizations). We also analyze the distribution of peak frequencies across individuals in Figure 2). Lower-pitched sounds characterize Peeps, while Twitters span a broader spectral range of peak frequencies. Notably, both call types exhibit bimodal distributions, with this pattern being more pronounced in certain individuals. This bimodal distribution could reflect two or more call subtypes with distinct pitches and should be investigated further to test for the existence of pragmatics or semantics in their communication system through pitch modulation. Variability within the Twitter call type extends beyond overall pitch modulation. Some Twitters exhibit an n-shaped pitch contour, a continuous descending note, a final lower-pitched note, or a

Table 1: Top-performing models for Twitters and Peeps (Mean F1 Score \pm SD), with significance assessed by comparison to the best simple model (Perch). Significance levels: * for $p < 0.05$ and ** for $p < 0.0001$ (Tukey’s test).

Model	F1 Score
Twitters	
Perch (Simple)	0.61 \pm 0.03
Whisper (Simple)	0.55 \pm 0.03
Perch + Whisper (Concat)	0.63 \pm 0.03
Perch + Whisper (Sum)	0.63 \pm 0.03*
Perch + Whisper (MRMR)	0.66 \pm 0.03**
Peeps	
Perch (Simple)	0.66 \pm 0.02
Whisper (Simple)	0.62 \pm 0.03
Perch + Whisper (Concat)	0.67 \pm 0.02*
Perch + Whisper (Sum)	0.68 \pm 0.02**
Perch + Whisper (MRMR)	0.70 \pm 0.02**

rising pitch throughout the call (Figure 1-A,B,C,D, respectively). Empirical studies incorporating rich social and environmental contexts will be crucial for uncovering the functional significance of this variation in Capuchin calls.

5 Conclusion

This study examined Acoustic Individual Identification in two call types of White-Faced Capuchins. We established performance baselines for pre-trained embeddings and found that combining multiple embeddings (summation, concatenation, and minimum redundancy maximum relevance) improves classification performance. Our findings also indicate that domain relevance outweighs model size in noisy environments. Future work should extend these multi-species embeddings to other taxa, confirming broader applicability in bioacoustics and animal linguistics.

6 Limitations

While this study focused on Acoustic ID, a deeper investigation into the behavioral and social functions of these call types remains relevant for future work. While there are other ways of improving Acoustic ID, such as data augmentation (MacIsaac et al., 2024), we considered those techniques out of scope for the present study and focused on investigating the complementarity of joint multi-species

embeddings. Our primary goal with this dataset is to make it accessible to the broader scientific community. We anticipate making it publicly available in a forthcoming study with further analyses.

7 Ethical Considerations

No animals were harmed during this study. All research adhered to ethical guidelines for animal welfare, recognizing the importance of studying animal communication while prioritizing their well-being, particularly in the context of climate change and habitat loss affecting this species. Additionally, all individuals involved in data collection and processing were engaged in formal employment or academic research under ethical labor practices.

References

Artem Abzaliev, Humberto Pérez Espinosa, and Rada Mihalcea. 2024. Towards dog bark decoding: Leveraging human speech processing for automated bark classification. *arXiv preprint arXiv:2404.18739*.

Alexei Baeviski, Henry Zhou, Abdelrahman Mohamed, and Michael Auli. 2020. *wav2vec 2.0: A framework for self-supervised learning of speech representations*. Preprint, arXiv:2006.11477.

Thore J Bergman, Jacinta C Beehner, Melissa C Painter, and Morgan L Gustison. 2019. The speech-like properties of nonhuman primate vocalizations. *Animal Behaviour*, 151:229–237.

Peter C Bermant. 2021. Biocppnet: automatic bioacoustic source separation with deep neural networks. *Scientific Reports*, 11(1):23502.

Mélicha Berthet, Camille Coye, Guillaume Dezechache, and Jeremy Kuhn. 2023. Animal linguistics: a primer. *Biological reviews*, 98(1):81–98.

Daniel L Bowling and W Tecumseh Fitch. 2015. Do animal communication systems have phonemes? *Trends in Cognitive Sciences*, 19(10):555–557.

Nora V Carlson, E McKenna Kelly, and Iain Couzin. 2020. Individual vocal recognition across taxa: a review of the literature and a look into the future. *Philosophical Transactions of the Royal Society B*, 375(1802):20190479.

Jules Cauzinille, Benoît Favre, Ricard Marxer, Dena Clink, Abdul Hamid Ahmad, and Arnaud Rey. 2024. Investigating self-supervised speech models’ ability to classify animal vocalizations: The case of gibbon’s vocal signatures. In *Interspeech 2024*, pages 132–136. ISCA; ISCA.

Dena J Clink, Hope Cross-Jaya, Jinsung Kim, Abdul Hamid Ahmad, Moeurk Hong, Roenun Sala, Hélène Birot, Cain Agger, Thinh Tien Vu,

Hoà Nguyen Thi, et al. 2024. Benchmarking automated detection and classification approaches for monitoring of endangered species: a case study on gibbons from cambodia. *bioRxiv*, pages 2024–08.

Margaret C Crofoot, Daniel I Rubenstein, Arun S Maiya, and Tanya Y Berger-Wolf. 2011. Aggression, grooming and group-level cooperation in white-faced capuchins (*cebus capucinus*): Insights from social networks. *American Journal of Primatology*, 73(8):821–833.

Chris Ding and Hanchuan Peng. 2005. Minimum redundancy feature selection from microarray gene expression data. *Journal of bioinformatics and computational biology*, 3(02):185–205.

Sabrina Engesser, Jodie MS Crane, James L Savage, Andrew F Russell, and Simon W Townsend. 2015. Experimental evidence for phonemic contrasts in a non-human vocal system. *PLoS biology*, 13(6):e1002171.

Burooj Ghani, Tom Denton, Stefan Kahl, and Holger Klinck. 2023a. Global birdsong embeddings enable superior transfer learning for bioacoustic classification. *Scientific Reports*, 13(1):22876.

Burooj Ghani, Tom Denton, Stefan Kahl, and Holger Klinck. 2023b. *Global birdsong embeddings enable superior transfer learning for bioacoustic classification*. *Scientific Reports*, 13(1):22876.

Zoë Goldsborough, Margaret C Crofoot, and Brendan J Barrett. 2024. Male-biased stone tool use by wild white-faced capuchins (*cebus capucinus* imitator). *American Journal of Primatology*, 86(4):e23594.

Julie J Gros-Louis, Susan E Perry, Claudia Fichtel, Eva Wikberg, Hannah Gilkenson, Susan Wofsy, and Alex Fuentes. 2008. Vocal repertoire of *cebus capucinus*: acoustic structure, context, and usage. *International Journal of Primatology*, 29:641–670.

Wei-Ning Hsu, Benjamin Bolte, Yao-Hung Hubert Tsai, Kushal Lakhotia, Ruslan Salakhutdinov, and Abdelrahman Mohamed. 2021. *Hubert: Self-supervised speech representation learning by masked prediction of hidden units*. Preprint, arXiv:2106.07447.

Po-Yao Huang, Hu Xu, Juncheng Li, Alexei Baeviski, Michael Auli, Wojciech Galuba, Florian Metze, and Christoph Feichtenhofer. 2023. *Masked autoencoders that listen*. Preprint, arXiv:2207.06405.

K. Lisa Yang Center for Conservation Bioacoustics at the Cornell Lab of Ornithology. 2024. *Raven pro: Interactive sound analysis software (version 1.6.5)*. [Computer software].

Stefan Kahl, Tom Denton, Holger Klinck, Hendrik Reers, Francis Cherutich, Hervé Glotin, Hervé Goëau, Willem-Pier Vellinga, Robert Planqué, and Alexis Joly. 2023. Overview of birdclef 2023: Automated bird species identification in eastern africa. In *CLEF (Working Notes)*, pages 1934–1942.

- 427 Stefan Kahl, Connor M. Wood, Maximilian Eibl, and
428 Holger Klinck. 2021. [Birdnet: A deep learning so-
429 lution for avian diversity monitoring](#). *Ecological
430 Informatics*, 61:101236.
- 431 Elly Knight, Tessa Rhinehart, Devin R de Zwaan,
432 Matthew J Weldy, Mark Cartwright, Scott H Hawley,
433 Jeffery L Larkin, Damon Lesmeister, Erin Bayne,
434 and Justin Kitzes. 2024. Individual identification in
435 acoustic recordings. *Trends in Ecology & Evolution*.
- 436 Konrad Lorenz. 1952. *King Solomon's Ring*. T. Y.
437 Crowell, New York.
- 438 Jennifer MacIsaac, Stuart Newson, Adham Ashton-Butt,
439 Huma Pearce, and Ben Milner. 2024. [Improving
440 acoustic species identification using data augmenta-
441 tion within a deep learning framework](#). *Ecological
442 Informatics*, 83:102851.
- 443 Marius Miron, Sara Keen, Jen-Yu Liu, Benjamin Hoff-
444 man, Masato Hagiwara, Olivier Pietquin, Felix Effen-
445 berger, and Maddie Cusimano. 2024. Biodenoising:
446 animal vocalization denoising without access to clean
447 data. *arXiv preprint arXiv:2410.03427*.
- 448 Anthony Miyaguchi, Adrian Cheung, Murilo Gustineli,
449 and Ashley Kim. 2024. Transfer learning with
450 pseudo multi-label birdcall classification for ds@ gt
451 birdclef 2024. *arXiv preprint arXiv:2407.06291*.
- 452 Susan E Perry, Brendan J Barrett, and Irene Godoy.
453 2017. Older, sociable capuchins (*cebus capucinus*)
454 invent more social behaviors, but younger monkeys
455 innovate more in other contexts. *Proceedings of the
456 National Academy of Sciences*, 114(30):7806–7813.
- 457 Alec Radford, Jong Wook Kim, Tao Xu, Greg Brock-
458 man, Christine McLeavey, and Ilya Sutskever. 2022.
459 [Robust speech recognition via large-scale weak su-
460 pervision](#). *Preprint*, arXiv:2212.04356.
- 461 Thom Scott-Phillips and Christophe Heintz. 2023. An-
462 imal communication in linguistic and cognitive per-
463 spective. *Annual Review of Linguistics*, 9(1):93–111.
- 464 PJB Slater. 1981. Individual differences in animal be-
465 havior. In *Perspectives in Ethology: Volume 4 Advan-
466 tages of Diversity*, pages 35–49. Springer.
- 467 Toshitaka N Suzuki. 2021. Animal linguistics: explor-
468 ing referentiality and compositionality in bird calls.
469 *Ecological Research*, 36(2):221–231.
- 470 Toshitaka N Suzuki. 2024. Animal linguistics. *Annual
471 Review of Ecology, Evolution, and Systematics*, 55.
- 472 Elizabeth Tinsley Johnson, Marcela E Benítez, Alexan-
473 der Fuentes, Celia R McLean, Arieck B Norford,
474 Juan Carlos Ordoñez, Jacinta C Beehner, and Thore J
475 Bergman. 2020. High density of white-faced ca-
476 puchins (*cebus capucinus*) and habitat quality in the
477 taboga forest of costa rica. *American Journal of Pri-
478 matology*, 82(2):e23096.
- Laurens van der Maaten. 2009. [Learning a parametric
embedding by preserving local structure](#). In *Inter-
national Conference on Artificial Intelligence and
Statistics*.

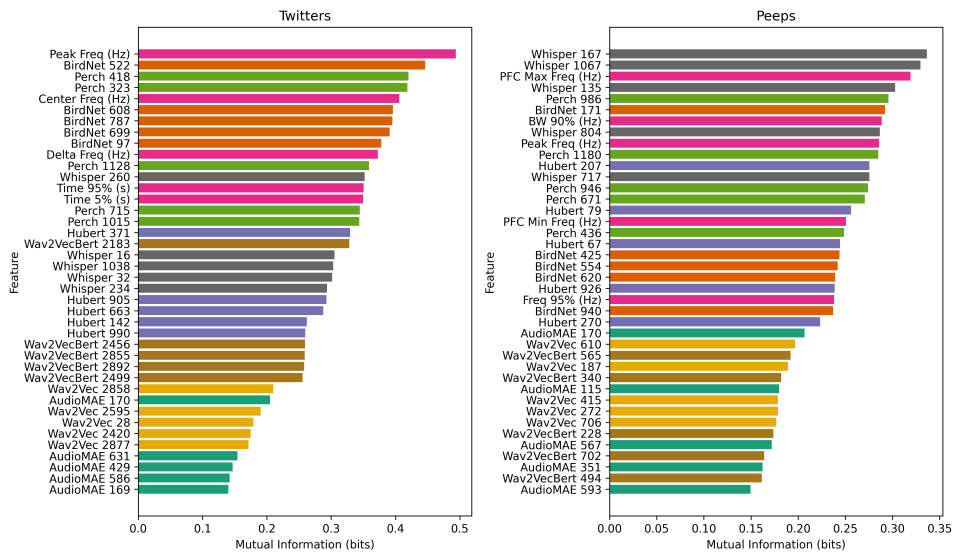


Figure 3: Mutual information of the top features for both call type datasets, spanning seven acoustic pre-trained embeddings. We display the five highest-performing features per pre-trained embedding, along with the top five interpretable features per model.

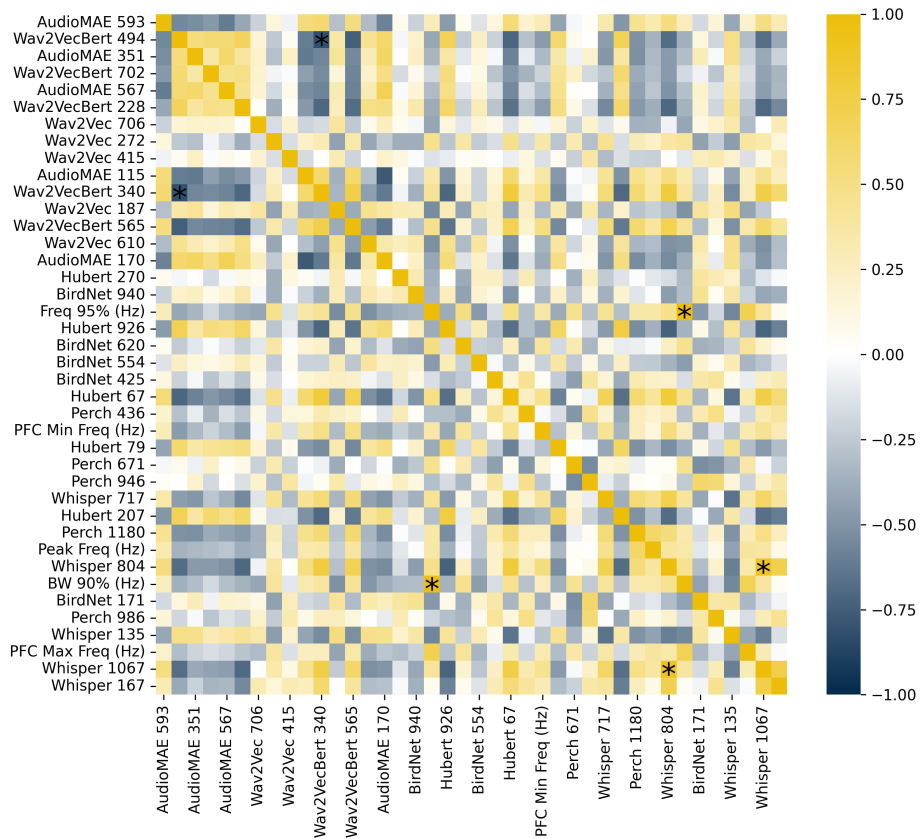


Figure 4: Mutual information of the top features in the Peeps call type dataset, spanning seven acoustic pre-trained embeddings. We display the five highest-performing features per pre-trained embedding, along with the top five interpretable features. Asterisks show correlation coefficients above 0.8.

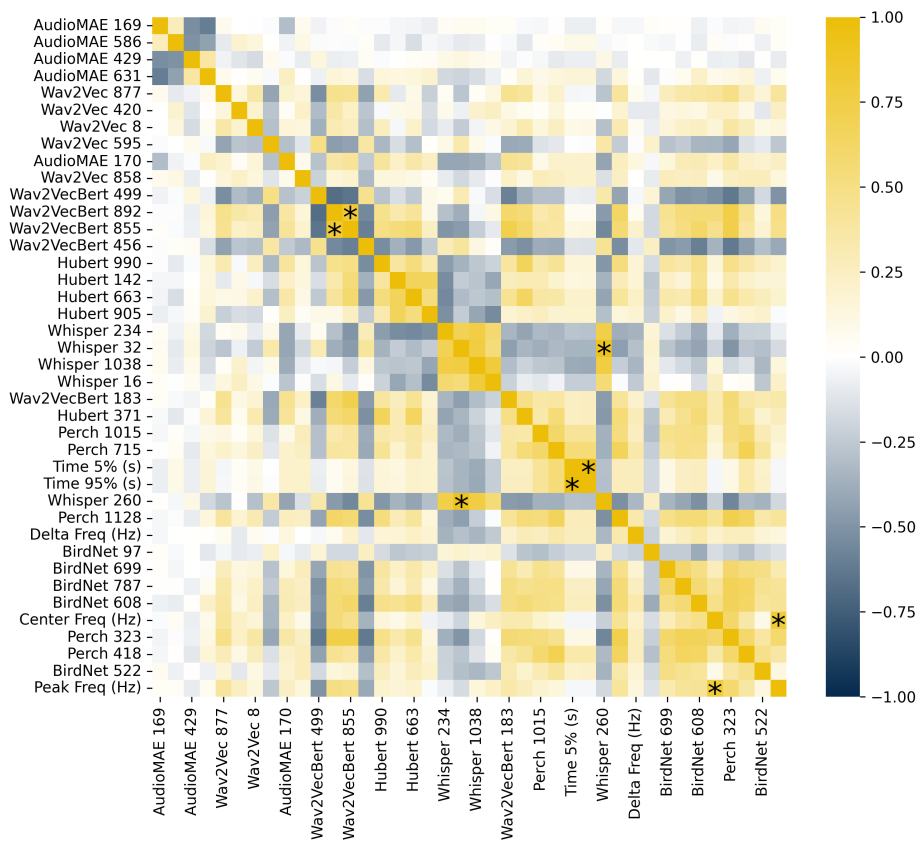


Figure 5: Mutual information of the top features in the Twitters call type dataset, spanning seven acoustic pre-trained embeddings. We display the five highest-performing features per pre-trained embedding, along with the top five interpretable features. Asterisks show correlation coefficients above 0.8.

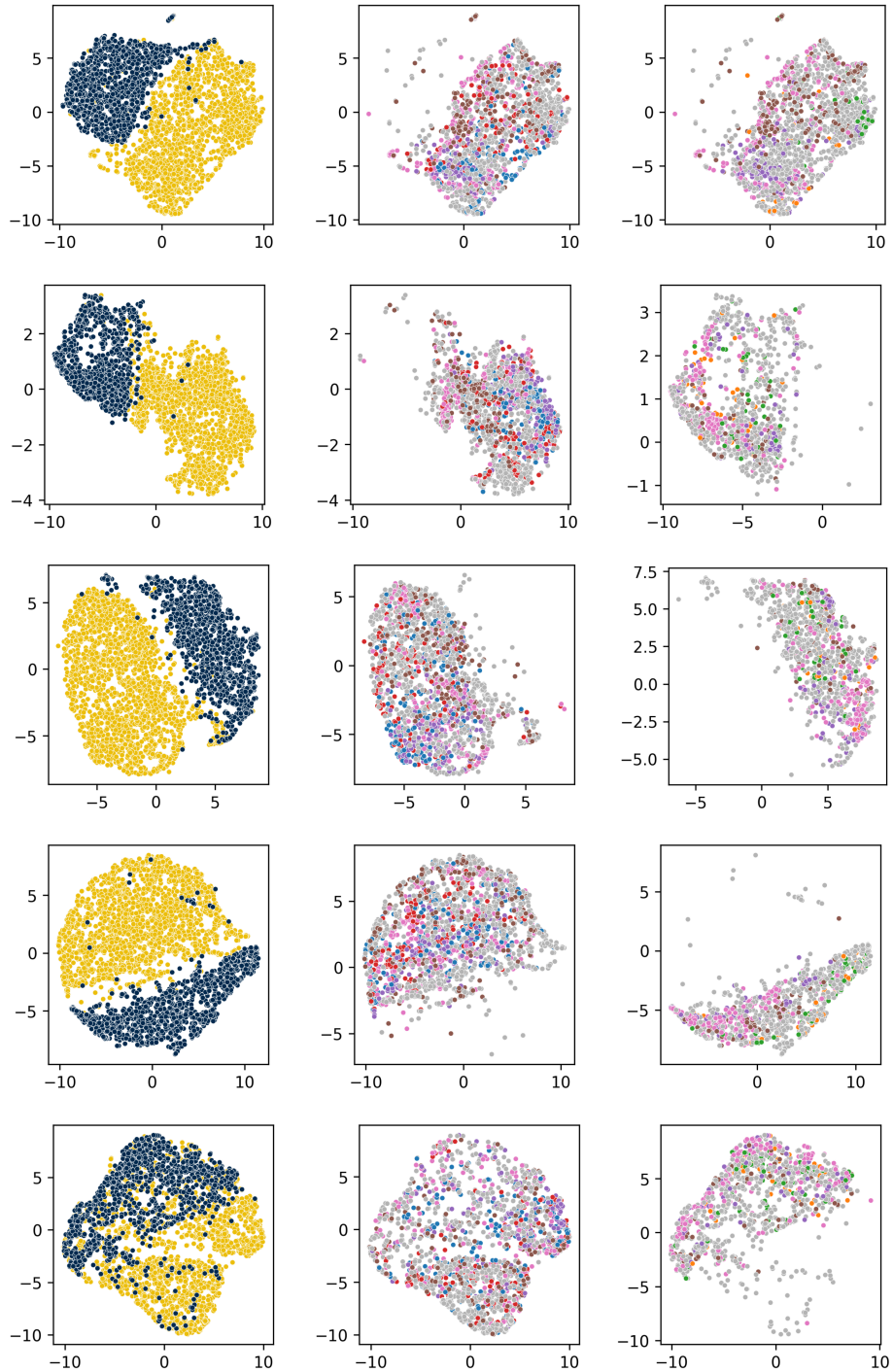


Figure 6: t-SNE visualizations of five pre-trained embeddings, primarily trained on human speech data (with AudioMAE also incorporating internet-sourced audio). The first column presents the t-SNE plot of call types (Peeps in yellow and Twitters in blue), while the second and third columns show the t-SNE projections of Twitters and Peeps, respectively, with points colored by individual identity. From top to bottom, the rows correspond to HuBERT, Wav2Vec, Wav2Vec BERT, Whisper, and AudioMAE.

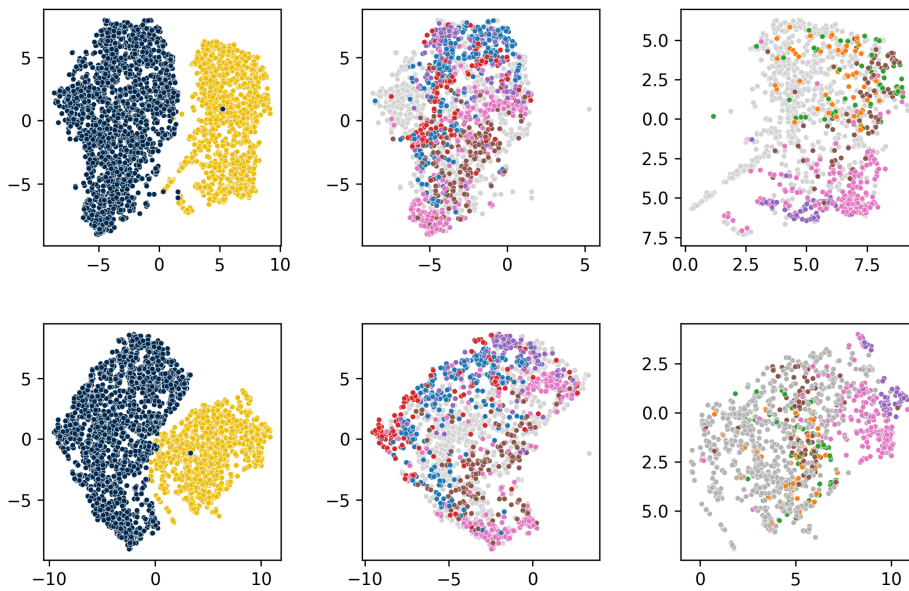


Figure 7: tSNE visualizations of five pre-trained embeddings, primarily trained on bioacoustics bird data (with BirdNET also incorporating other animals). The first column represents the t-SNE plot of call types (Peeps in yellow and Twitters in blue), while the second and third columns depict the t-SNE projections of Twitters and Peeps colored by individual, respectively. From top to bottom, the rows correspond to BirdNET and Perch, respectively.

Model	F1 Score (Mean \pm Std)
Simple Network	
Perch	0.66 \pm 0.02
Whisper	0.62 \pm 0.03
BirdNet	0.60 \pm 0.02
HuBERT	0.55 \pm 0.02
Wav2Vec2	0.47 \pm 0.02
Concatenation (2 Embeddings)	
BirdNET + Perch	0.67 \pm 0.02
Perch + Whisper	0.67 \pm 0.02
Perch + Hubert	0.66 \pm 0.02
Perch + AudioMAE	0.64 \pm 0.02
Perch + Wav2Vec2	0.64 \pm 0.02
Summation (2 Embeddings)	
Perch + Whisper	0.68 \pm 0.02
Perch + BirdNET	0.67 \pm 0.02
Perch + HuBERT	0.66 \pm 0.02
BirdNet + Whisper	0.64 \pm 0.02
Perch + Wav2Vec2	0.64 \pm 0.02
MRMR (2 Embeddings)	
Perch + Whisper	0.70 \pm 0.02
Perch + BirdNET	0.69 \pm 0.02
Perch + HuBERT	0.68 \pm 0.02
Perch + Wav2Vec2	0.67 \pm 0.02
Perch + Wav2Vec-bert	0.67 \pm 0.02

Table 2: Performance of the top 5 models per method on the Acoustic ID task using the Peeps dataset (Mean F1 Score \pm Standard Deviation).

Model	F1 Score (Mean \pm Std)
Simple Network	
Perch	0.61 \pm 0.03
BirdNet	0.60 \pm 0.04
HuBERT	0.56 \pm 0.04
Whisper	0.55 \pm 0.03
Wav2Vec-bert	0.43 \pm 0.03
Concatenation (2 Embeddings)	
BirdNET + Whisper	0.63 \pm 0.03
BirdNET + Perch	0.62 \pm 0.03
Perch + Whisper	0.62 \pm 0.03
BirdNET + HuBERT	0.62 \pm 0.03
Perch + HuBERT	0.61 \pm 0.03
Summation (2 Embeddings)	
BirdNET + Whisper	0.63 \pm 0.04
Perch + Whisper	0.63 \pm 0.03
BirdNET + Perch	0.63 \pm 0.03
BirdNET + HuBERT	0.62 \pm 0.03
Perch + HuBERT	0.62 \pm 0.03
MRMR (2 Embeddings)	
Perch + Whisper	0.66 \pm 0.03
BirdNET + Whisper	0.65 \pm 0.03
Perch + HuBERT	0.64 \pm 0.03
BirdNET + Perch	0.64 \pm 0.03
Perch + Wav2Vec2	0.64 \pm 0.03

Table 3: Performance of the top 5 models per method on the Acoustic ID task using the Twitters dataset (Mean F1 Score \pm Standard Deviation).

Measurement	Units	Definition
Center Freq	Hz	The frequency that divides the selection into two intervals of equal energy (i.e., the 50th percentile frequency) measured on each spectrogram slice.
Freq 25%	Hz	The 25th percentile frequency (first quartile) measured on each spectrogram slice.
Freq 75%	Hz	The 75th percentile frequency (third quartile) measured on each spectrogram slice.
Freq 5%	Hz	The 5th percentile frequency measured on each spectrogram slice, indicating the lower bound of the energy distribution.
Freq 95%	Hz	The 95th percentile frequency measured on each spectrogram slice, indicating the upper bound of the energy distribution.
BW 50%	Hz	The inter-quartile range bandwidth, computed as the difference between the 75th and 25th percentile frequencies (i.e., the bandwidth containing 50% of the energy).
BW 90%	Hz	The bandwidth encompassing 90% of the signal's energy, calculated as the difference between the 95th and 5th percentile frequencies.
Peak Freq	Hz	The frequency at which the maximum power (or peak power) occurs within the selection, as observed in each spectrogram slice.
Center Time	s	The time that divides the selection into two intervals of equal energy (i.e., the median or 50th percentile time) for the signal's energy distribution.
Time 25%	s	The time by which 25% of the total energy has been accumulated within the selection.
Time 75%	s	The time by which 75% of the total energy has been accumulated within the selection.
Dur 50%	s	The duration over which the central 50% of the signal's energy is distributed, computed as the difference between the 75th and 25th percentile times.
Time 5%	s	The time by which 5% of the total energy has been accumulated within the selection.
Time 95%	s	The time by which 95% of the total energy has been accumulated within the selection.
Dur 90%	s	The duration over which 90% of the signal's energy is distributed, computed as the difference between the 95th and 5th percentile times.
Delta Freq	Hz	The difference between the upper and lower frequency limits of the selection.
Delta Time	s	The difference between the beginning and ending times of the selection.
Time 5% Rel.	–	The relative time (as a proportion of total duration) at which 5% of the signal's energy is accumulated.
Time 25% Rel.	–	The relative time at which 25% of the signal's energy is accumulated.
Center Time Rel.	–	The relative time corresponding to the median (50%) of the signal's energy distribution.
Time 75% Rel.	–	The relative time at which 75% of the signal's energy is accumulated.
Time 95% Rel.	–	The relative time at which 95% of the signal's energy is accumulated.
Peak Time Relative	–	The time at which the peak amplitude occurs, expressed as a proportion of the total selection duration.
PFC Avg Slope	Hz/ms	The average slope of the peak frequency contour over time, computed as the mean of the differences between successive peak frequencies.
PFC Max Freq	Hz	The maximum frequency reached in the peak frequency contour.
PFC Max Slope	Hz/ms	The maximum rate of change (slope) observed in the peak frequency contour.
PFC Min Freq	Hz	The minimum frequency reached in the peak frequency contour.
PFC Min Slope	Hz/ms	The minimum rate of change (slope) observed in the peak frequency contour.
PFC Num Inf Pts	–	The number of inflection points in the peak frequency contour, indicating how frequently the slope changes sign.

Table 4: Summary of acoustic measurements derived from Raven Pro 1.6. Definitions are adapted from the Raven Pro manual.

Model name	Number of parameters	Training data (hours)	Reference
BirdNET	27M	8300	Kahl et al. (2021)
Hubert-Large	1B	60960	Hsu et al. (2021)
Perch	7.8M	<10k	Ghani et al. (2023b)
Wav2vec2	317M	54000	Baevski et al. (2020)
W2v-BERT 2.0	600M	60960	Hsu et al. (2021)
Whisper-Large-v2	1.55B	680000	Radford et al. (2022)
AudioMAE	304M	5500	Huang et al. (2023)

Table 5: List of considered models for acoustic embeddings, including their size, training data, and references.